Effects of lifting reactance requirements on the optimal design of converter-fed synchronous hydrogenerators

Erlend L. Engevik, *Member, IEEE,* Truls E. Hestengen,
Mostafa Valavi, *Member, IEEE,* and Arne Nysveen, *Senior Member, IEEE*
Department of Electric Power Engineering, Norwegian University of Science and Technology (NTNU)
Trondheim, Norway, erlend.engevik@ntnu.no

***Abstract*—The maximum allowed per unit value of the synchronous reactance of a synchronous generator is normally decided by the grid codes in order to maintain the stability of the system. For the converter-fed synchronous hydrogenerator, the steady state stability can be maintained by the frequency converter. In this paper the constraint on the synchronous reactance is relaxed from 1.2 per unit to 2.0 per unit and then removed altogether. The cost of the active materials and the net present value of the cost of losses are calculated for each case and compared. Three different nominal frequencies are also used to find which one gives the lowest total cost. The total generator cost is reduced when the synchronous reactance is increased. The lowest cost of the 50 Hz designs are lower than the cost of the 25 and 75 Hz designs.**

***Index Terms*—Converter-fed Synchronous Machine (CFSM), Electrical Machine Design, Genetic Algorithms (GA), Hydropower, Losses, Reactance, Variable Speed**

NOMENCLATURE

A	Armature loading (A/cm).
A_p	Pole surface area (m^2).
b_{cuf},b_{pc}	Field winding width, Pole core width (mm).
B_δ	Peak airgap flux density (T).
b_u	Width of stator slot (mm).
C	Cost coefficient (€/kg, €/kW).
D,D_o	Stator bore, outer diameter (m).
δ	Airgap length (mm).
I_s,I_f	Stator and field current (A).
k_{cs}, k_w	Carter's coefficient due to slotting and total winding factor.
L	Stator core length (m).
$m_{cu,r/s}$	Weight of rotor/stator copper (tonne).
$m_{Fe,r/s}$	Weight of rotor/stator iron (tonne).
n, n_s	Rotational speed, s for synchronous (rpm).
P_{cus}	Stator copper losses (kW).
P_{r+exc}	Rotor copper and exciter losses (kW).
P_{Fe}	Total stator iron losses (kW).
P_{add}, P_{fw}	Additional and mechanical losses (kW).
P_{ps}	Pole shoe losses,nl-no load,fl-full load (kW).
Q_s	Number of stator slots.
τ_s	Stator slot pitch (mm).
U_n	Stator line voltage (kV).
X_{ad}	Armature reaction reactance (p.u.).
X_d, X'_d	Synchronous and transient reactance (p.u.).
X''_d	Subtransient reactance (p.u.).

This work was supported by Norwegian Hydropower Centre (NVKS).

I. INTRODUCTION

Synchronous hydrogenerators today are designed to be directly grid connected. They are constrained by the existing grid codes at the sites where they have been installed. One of the limiting design constraints given by these grid codes is the stability demand that directly affects the allowed value of the synchronous reactance of generators.

In applications like pumped storage, where variable speed operation of the generator is desirable, the converter-fed synchronous generator topology (CFSM) seems to be the most promising [1]. With the CFSM, the generator is decoupled from the grid by the converter. Therefore the requirement on the synchronous reactance can be lifted in order to reduce the total cost. The purpose of this paper is to investigate how lifting the reactance requirement affects the design and cost of the optimized generator. This is done primarily by changing the airgap length.

The limiting value for the synchronous reactance is mainly met by adjusting the airgap length in the machine. A low maximum value for the synchronous reactance requires a longer airgap and more ampere-turns in the field winding for the same apparent power [2]. This gives more field current and field winding losses, tougher cooling requirements and lower generator efficiency [3]. By lifting the upper limit for the synchronous reactance, the airgap length is allowed to go down.

Subject to synchronous reactance constraints, the length of the airgap is dimensioned to optimize the efficiency by minimizing the magnetizing current [4].

Flux harmonics in the airgap are caused by tooth ripple and stator winding spatial harmonics that induce losses in the rotor pole surface and in damper windings [5].

A reduction in airgap length is accompanied by an increase in pole surface losses due to a larger slot width to airgap ratio. In order to keep heating due to pole surface losses low, the

978-1-5090-4281-4/17/$31.00

airgap should be kept large enough to have a low slot width to airgap ratio [6].

In converter-fed machines there are additional losses on top of those induced by spatial harmonics in the airgap. These losses are caused by time harmonics in the supply voltage.

In [7] it was found that there can be a significant increase in rotor surface and damper winding losses for the same machine if one change the supply voltage from sinusoidal to pulse width modulated-type. This indicates that in the cases where surface losses become significant for sinusoidal supply, they will most likely be more severe for a converter-fed machine.

II. Optimization model

A. Problem formulation

Genetic algorithms (GA) are population based, evolutionary algorithms which follow the principles of reproduction, natural selection, and diversity. GAs are one of the most widely used families of stochastic optimization methods in electrical machine design. Using the GA, one is never assured to find the exact global optimum but one can get really close. More details on the implementation of GA as it is used in this paper are given in [8] where a hybrid version of the GA was used. In the hybrid version, a gradient optimization method was used as a final stage after the GA had found the optimal area of the solution space. In this paper, the hybrid version is not used, only the GA.

All the results presented in this paper are the average of 10 runs of the same configuration. This is done in order to even out some of the variation that comes with using GA as the chosen optimization method.

Design specifications are given in Table I. Variables used in the optimization together with upper and lower bounds are given in Table II. The bounds on each variable are set to give a design space that is sufficiently large while at the same time give reasonable values.

TABLE I:
Design specifications

S_N	Rated apparent power	105 MVA
$cos(\phi)$	Power factor	0.9
N_{ph}	Number of phases	3
N_b	Number of parallel circuits	2
n_s	Synchronous speed	375 rpm

B. Constraints and limitations

Constraints are presented in Table III. The synchronous reactance X_d is initially limited to maintain static stability for the generator. A typical upper limit for the synchronous reactance for hydropower generators is 1.2 p.u. Additionally, the transient reactance should not be above 0.4 p.u. The subtransient reactance is important for limiting the short circuit currents and to prevent failures from spreading to other parts of the power system. A lower limit of 0.15 p.u. was implemented for the subtransient reactance.

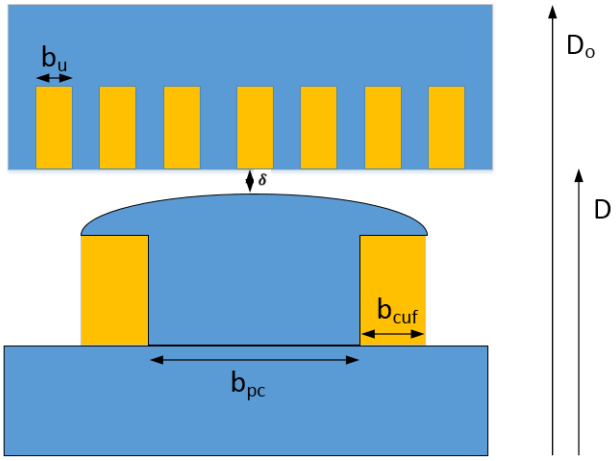

Fig. 1: Geometric variables, parameters explained in the nomenclature

TABLE II:
Independent machine variables

		lower	upper
Q_{ss}	Number of stator slots divided by 6	13	65
D	Stator bore (m)	2	7
n_v	Number of cooling ducts	20	60
b_u	Width of stator slot (mm)	10	40
n_{str}	Number of strands per stator slot	20	120
b_{pc}	Pole core width (mm)	200	900
n_f	Number of turns per pole	30	200
b_{cuf}	Width of field winding (mm)	50	300
δ	Airgap length (mm)	0	60
h_{cus}	Height of Roebel bar strand (mm)	1.5	2.5
h_{cuf}	Height of field winding turn (mm)	4.0	5.0

Current density needs to be limited to prevent overheating in both stator and rotor. Common values range from 2 to 5 $\mathrm{A/mm^2}$. An upper limit of 5 $\mathrm{A/mm^2}$ is implemented for the stator and rotor current density J_s and J_f. The maximum ac to dc resistance factor of the stator winding is set to 1.5 for the same reason. In addition the Roebel bars are checked to ensure that a full transposition is possible within each stack length.

In order to estimate the temperature rise in the different parts of the generator, a thermal equivalent circuit network similar to the one presented in [9] was used. Design parameters like diameter, axial length, reactances and the weight of the different parts of the generator are calculated using the analytical framework presented in [10]. Magnetic calculations are based on a magnetic equivalent circuit representation similar to the one given in [9].

According to [11] the mechanical starting time, i.e. the time it takes to accelerate the rotor from standstill to rated speed using nominal torque, is given as $T_M = 2 \cdot H$. For

TABLE III:
Parameter constraints

Parameter	Constraint
Slot width	$\geq 0.8 \cdot \tau_s$
Pole clearing	$\geq$ 2 mm
Synchronous reactance*	$\leq$ 1.2 p.u.
Transient reactance	$\leq$ 0.4 p.u.
Subtransient reactance	$\geq$ 0.15 p.u.
Tooth flux density	$\leq$ 1.7 T
Pole core flux density	$\leq$ 1.6 T
Rotor yoke flux density	$\leq$ 1.3 T
Stator current density	$\leq$ 5 A/mm^2
Rotor current density	$\leq$ 5 A/mm^2
Rotor tip speed at runway speed	$\leq$ 150 m/s
Inertia constant $\frac{T_M}{T_w}$	$\geq$ 4

* - initial value

large generators connected to the grid, the system operator often specifies restrictions to its moment of inertia. This is to maintain enough inertia in the power system which preserves the system stability. Statnett, the Norwegian system operator says in the Norwegian grid codes for transmission system [12] that the ratio between the time constants for the moment of inertia T_M and the water way T_w should be more than 4. T_w is usually set to 1s [13].

C. Objective function

In order to optimize both cost and efficiency at the same time, without using multiple objective functions, the cost of the generator is chosen as the objective function. In the cost function, (1), both material costs and the net present value of the cost of losses are included. Cost of losses are divided into load dependent losses (P_{ld}) and constant losses (P_{cons}). The constant losses are assumed to be iron losses, mechanical losses, exciter losses and rotor copper losses at no-load. Load dependent losses are assumed to be stator copper losses, rotor copper losses at load and additional losses.

$$\begin{aligned} C_{tot} =& C_{ld} \cdot P_{ld} + C_{cons} \cdot P_{cons} + C_{steel} \cdot m_{Fe,r} \\ &+ C_{lam} \cdot m_{Fe,s} + C_{cu} \cdot (m_{cu,s} + m_{cu,r}) \end{aligned} \tag{1}$$

Prices for the different materials are based on typical values similar to values used in other publications [14]. The unit prices for the active materials that are used are:

- stator iron C_{lam}: 4 €/kg
- rotor iron C_{steel}: 6 €/kg
- copper C_{cu}: 11 €/kg

For the losses, it is assumed that the generator is not run as a base plant at nominal power output all the time. The cost of losses may vary from market to market. In this paper the cost of constant losses are set to 3000 €/kW, while the cost of load dependent losses are set to 2000 €/kW.

D. Main dimensions

The main dimensions of a salient pole synchronous generator is given by (2). The rated speed of rotation n_s, the airgap flux density B_δ and the armature current loading A sets the required airgap volume D^2L required to produce sufficient torque for the required active and apparent power S.

$$S = U_n I_s = \frac{\pi^2}{\sqrt{2}} k_w A B_\delta D^2 L n_s \tag{2}$$

For a fixed rotational speed and apparent power, an increase in A or B_δ leads to a reduction in the required airgap volume. The stator voltage U_n is mainly set by the limit on stator current I_s. k_w is the winding factor of the fundamental frequency, and is kept between 0.915 and 0.925 for all the cases investigated in this paper.

E. Losses

Generator losses are calculated using the formula presented in [10]. In addition to iron losses in the stator, copper losses in rotor and stator and mechanical losses, rotor surface losses and damper winding losses are calculated.

Rotor surface losses can be divided into losses caused by the tooth ripple in the stator and winding harmonics. These losses can be estimated using (3) given in [13]. P_{psnl} is the pole shoe losses at no-load due to slot openings where $\frac{Q_s n_s}{60}$ is the frequency (f) of the induced losses. One can see that the losses are proportional to $f^{1.5}$, taking both eddy current and hysteresis losses into account.

$$\begin{aligned} P_{psnl} &= 232 \Delta \left[(k_{cs} - 1) B_\delta \tau_s \right]^2 N_p A_p \left(\frac{Q_s n_s}{60} \right)^{1.5} \\ P_{psfl} &\approx K' \left(\frac{1}{(k_{cs} - 1)} \frac{N_p}{Q_S} \cdot X_{ad} \right)^2 P_{psnl} \\ P_{ps} &= P_{psnl} + P_{psfl} \end{aligned} \tag{3}$$

$K^{'} = 0.2$ is a parameter that takes into account the fact that the airgap is longer at the sides of the pole face. Δ is the thickness of the pole shoe laminations, set to 2 mm. The stator mmf also interacts with the tooth ripple harmonics in the airgap permeance to induce losses (P_{psfl}) in the pole surface and damper cage. In addition there will be losses due to other mmf harmonics, e.g. 3rd, 5th, 7th, 11th multiple of the main harmonic. A time-stepping finite element analysis should be performed in order to calculate these losses more accurately.

F. Model verification

Reactance calculations were compared with measurements from three existing hydrogenerators using design specifications given in [15]. The generators have power ratings of 36, 52 and 320 MVA respectively. The results are given in Table IV. The calculated values are somewhat lower than the measured values for generator G2. For G3 and G5, the synchronous and subtransient reactances calculated matches well with the

measured values. For the transient reactances, the calculated values seems to consistently be lower than the measured values.

TABLE IV:
Comparison between calculated and measured reactance values from [15]

	G_2		G_3		G_5	
Symbol	M	C	M	C	M	C
X_d	0.98	0.83	0.96	0.97	1.25	1.28
X'_d	0.32	0.26	0.30	0.24	0.27	0.24
X''_d	0.24	0.20	0.20	0.19	0.17	0.18
M - measured value			C - calculated value			

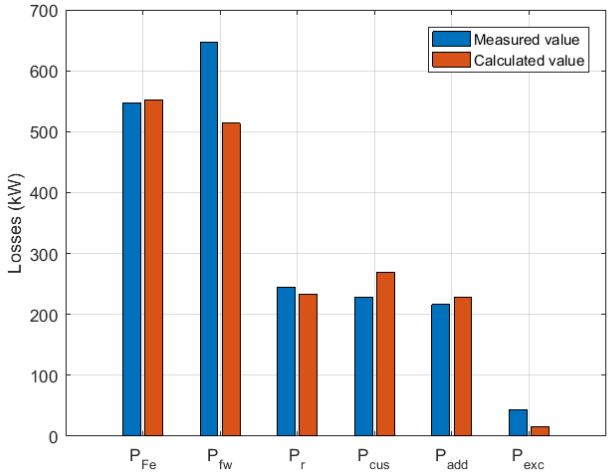

Fig. 2: Comparison between calculated and measured losses for 122.6 MVA hydrogenerator presented in [4].

In order to compare the loss calculations made to real loss data, the 122.6 MVA generator presented in [4] was used. Design data for the generator were used to calculate the losses with the analytical methodology that is used for all calculations in this paper. Results are presented and compared to the measured values in Fig. 2. Calculated losses seems to match well with the measured data. One exception is the estimation of the mechanical losses P_{fw}, which are difficult to estimate using the semi-experimental expressions that are given in various textbooks.

III. Results

When a converter-fed synchronous hydrogenerator is used, the nominal frequency is not fixed by the grid. Three different nominal frequencies, i.e. 25, 50 and 75 Hz, are used to see how the choice of nominal frequency affects the design and the total cost of the generator.

In order to investigate how lifting the requirement on the synchronous reactance affects the total cost of the generator, the total cost have been calculated for several upper limits. Initially, the value was set to 1.2 p.u. Then the limit was lifted to 2.0 p.u., and finally it was removed altogether.

When the limit on the synchronous reactance is removed, the reactance is allowed to be optimized for each frequency. For the 25 Hz designs, the optimal value was found to be 3.3 p.u. The optimal values were found to be 2.9 p.u. for the 50 Hz designs and 2.5 for the 75 Hz designs.

The main results of this paper are presented in Fig. 3(a). Two conclusions can be made:

1) the total generator cost is reduced when the synchronous reactance is increased.
2) the lowest cost of the 50 Hz designs are lower than the cost of the 25 and 75 Hz designs.

For the 75 Hz designs, which are the most expensive category, the cost is reduced by 4.49 % when the synchronous reactance is increased from 1.2 p.u. to 2 p.u. When the reactance value is allowed to rise even higher, the cost reduction is 0.56 %. For the 25 Hz designs the cost reductions are 5.62 % and 2.12 % respectively. For the least expensive designs, running at 50 Hz, the reductions are 5.02 % and 1.49 %.

Increasing the nominal frequency from 25 to 50 Hz reduces the cost of the generator 2.13 %, 1.51 % and 0.87 % respectively for the different reactance values. Increasing the frequency from 50 to 75 Hz shows an increase in total cost of 6.68 %, 7.95 % and 9.66 % respectively.

In [10] it is shown that the weight of the generator is reduced when the nominal frequency is increased. A higher nominal frequency gives a lighter generator with a lower cost for the active materials. The losses in the machine increase when the nominal frequency increase, increasing the cost of losses.

In Fig. 3(a),(b) and (c), the distribution of cost between losses and materials are presented for the different synchronous reactance values and nominal frequencies. The reason for the 50 Hz designs being cheaper than the 25 Hz designs, which in turn show to be cheaper than the 75 Hz designs, is revealed:

1) The cost of losses is increasing evenly for each increase in nominal frequency.
2) Material cost does not show the same trend.
   a) Moving from 25 Hz to 50 Hz results in a substantial decrease in the cost of materials.
   b) Moving from 50 Hz to 75 Hz only yields a smaller decrease in the cost of materials.
3) The 50 Hz designs being cheaper than the 25 Hz designs as the reduction in material costs are larger than the increase in cost of losses.
4) For the 75 Hz case the increase in cost of losses are larger than the reduction in cost of materials.
5) The 75 Hz designs are the most expensive options analysed.

When the nominal frequency increase, the cost of materials become smaller compared to the cost of losses. At higher frequencies the cost of losses start to dominate the total cost of the generator. At 25 Hz the material cost is 59 - 62 % of

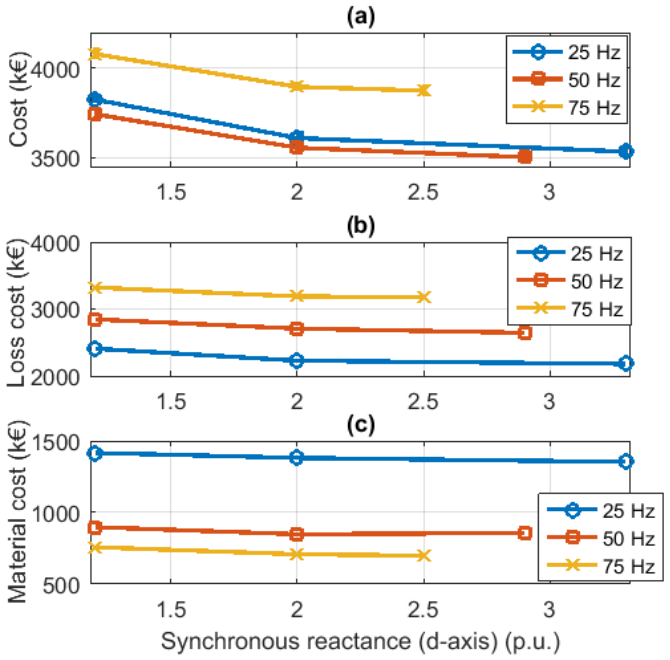

Fig. 3: Comparison of material and loss cost for different frequencies, (a) total cost, (b) loss cost, (c) material cost.

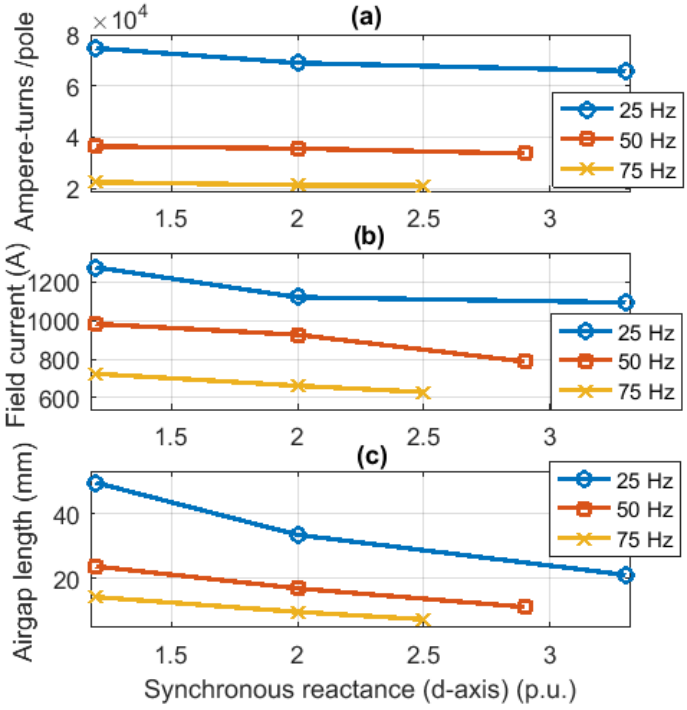

Fig. 4: Magnetization of the generator, (a) ampere-turns per pole, (b) field current, (c) airgap length.

the cost of losses. This ratio drops to 31-32 % at 50 Hz and 22 - 23 % at 75 Hz.

Fig. 4(a) gives the relationship between required magnetization, (b) field current and (c) the airgap length. One can see that the total ampere-turns per pole and the field current decreases when the airgap gets smaller. In [10] it is shown that the synchronous reactance is inversely proportional to the number of poles and the airgap length. Since the speed of rotation is constant, the number of poles must increase to increase the frequency. Increasing the number of poles or the value of the synchronous reactance necessitates a reduction in airgap length.

An increase in the synchronous reactance, reduces the required magnetization (ampere-turns), resulting in a reduction in field current. By lowering the field current, 4(b), the rotor losses goes down, Fig. 10(a). Less losses in the rotor gives less heating of the cooling air before it enters the stator. This allows the armature loading, see Fig. 5(b) to increase. The reason for this is that the air that enters the stator is colder, which make a higher temperature increase in the air that passes the stator winding possible. When the stator current increase, Fig. 6(b), the stator voltage is reduced, Fig. 6(a).

Increasing the armature loading A reduces the magnetic loading B_δ, Fig. 5(a). According to (2), when the product of A and B_δ goes up, the required volume of the machine D^2L goes down, see Fig. 7(c). This leads to a shorter machine ,Fig. 7(b). As the diameter is mainly determined by the number of poles [10], and the length L is reduced, the weight of iron in the rotor and stator goes down, Fig. 8(a).

The geometry of two optimized 50 Hz generators are presented in Fig. 9. One can see that the 2.0 p.u. synchronous reactance generator has a shorter airgap, thinner stator and rotor yokes and higher number of stator slots. The generator with 2.0 p.u. synchronous reactance has a higher number of stator slots that increases the armature loading in the machine. The main parameters of the two generators are presented in Table V. One can see that the armature loading is higher for the 2.0 p.u. generator, and that the weight of rotor and stator iron is reduced when the synchronous reactance is increased.

Losses in the generator are presented in Fig. 10. It can be seen that both iron losses and mechanical losses goes down when the synchronous reactance is increased. This can be attributed to the reduction in axial length as a result of the increased armature loading. From (2) we have that when A is increased, the necessary length L goes down. Mechanical losses increase with increasing frequency as a consequence of a larger generator diameter. For the 50 Hz designs, the increased diameter has a larger effect on the mechanical losses than the shorter length has.

Rotor losses are reduced when the synchronous reactance or the frequency is increased. This is both due to the reduction in field current mentioned earlier and because of an increase in the copper cross section giving a reduced field winding resistance. Additional losses increase when the airgap length is reduced due to more losses in the pole shoes.

Fig. 11(b) presents the relationship between pole shoe losses and the ratio of airgap length to slot opening. This figure indicates that poles shoe losses are kept small when the airgap

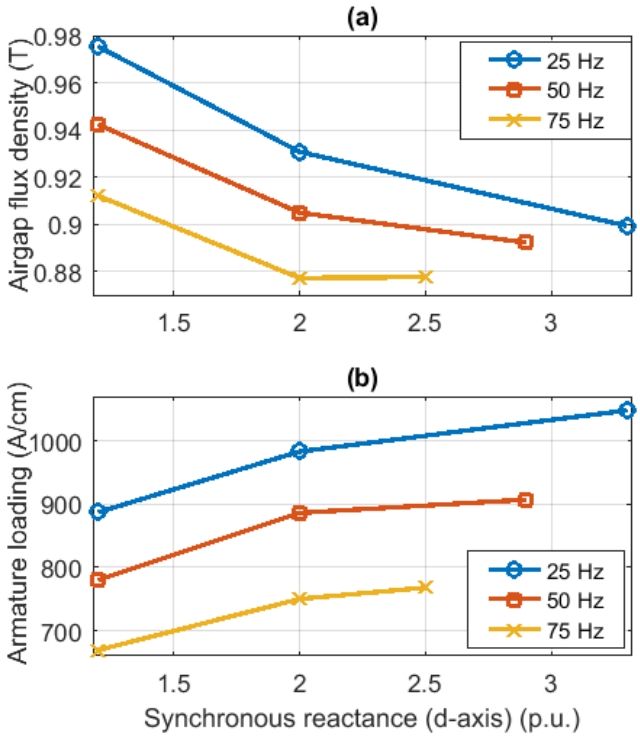

Fig. 5: Loading of the generator, (a) magnetic loading, (b) electric loading.

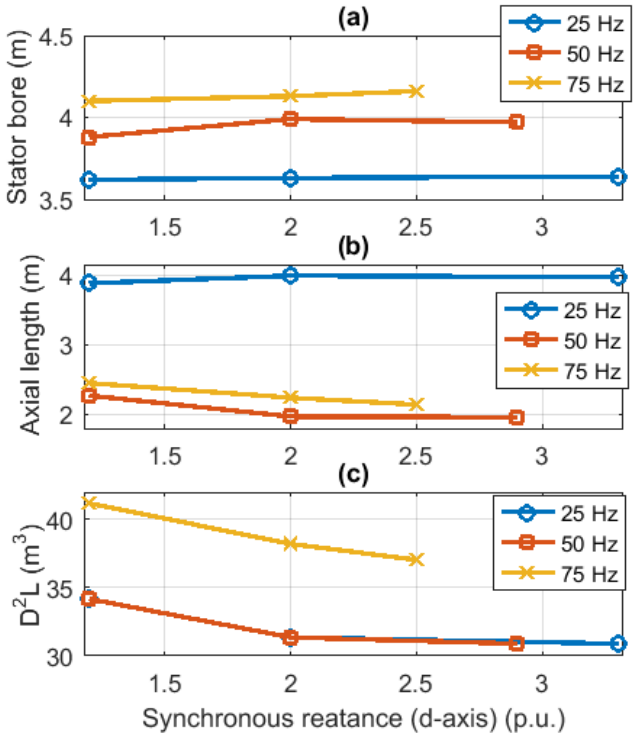

Fig. 7: Main dimensions of the generator, (a) stator bore, (b) axial length, (c) rotor volume.

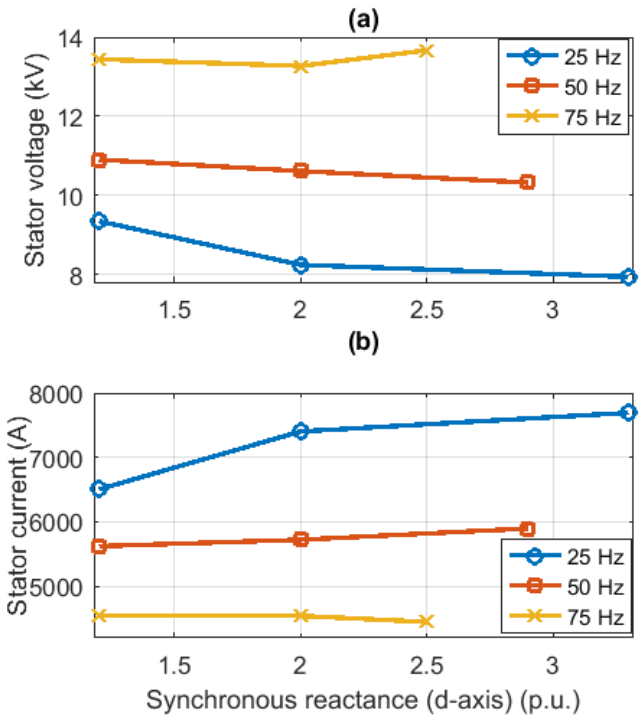

Fig. 6: Stator voltage (a) and stator current (b).

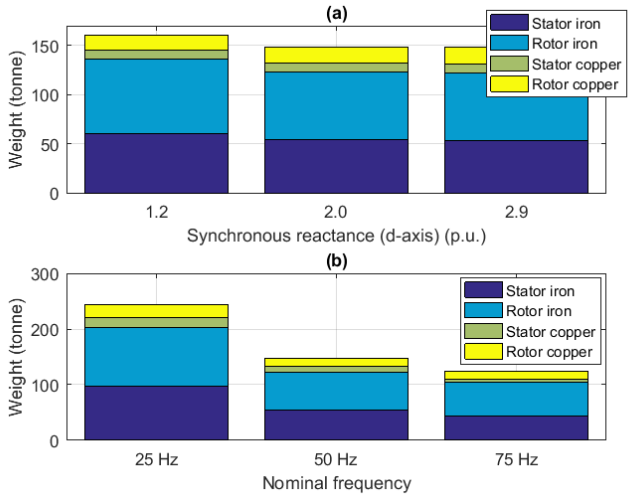

Fig. 8: Weight of the generator, (a) at 50 Hz, (b) at 2.0 p.u. synchronous reactance.

length to slot opening ratio is kept below 1.0.

Airgap length to slot opening is reduced when the synchronous reactance or nominal frequency is increased, see Fig. 11(a). The main reason for this is that the length of the airgap is reduced when the nominal frequency or the synchronous reactance is increased.

Pole shoe losses are increased to more than 50 kW at the smallest airgap length to slot opening ratio. When this ratio is

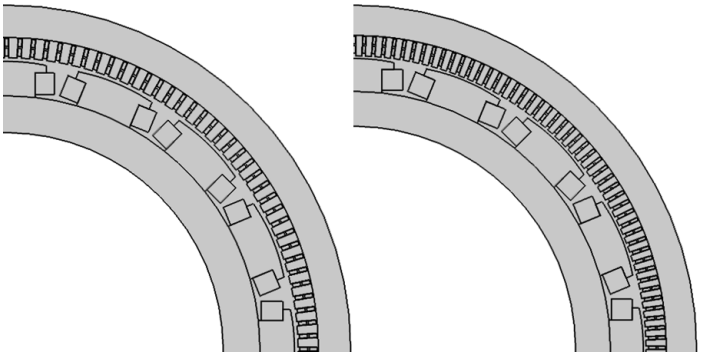

Fig. 9: Geometries of two 50 Hz generators. Left: 1.2 p.u. synchronous reactance. Right: 2.0 p.u. synchronous reactance.

TABLE V:
Design results from optimization (50 Hz)

	Synchronous reactance	1.2 p.u.:	2.0 p.u.:
	Cost	3699.6 k€	3535.9 k€
	Total weight	162076 kg	144594 kg
	Independent variables:		
Q_s	Number of stator slots	144	192
D	Stator bore (m)	3.85	4.03
n_v	Number of cooling ducts	50	41
b_u	Width of stator slot (mm)	28.8	24.8
n_{str}	Number of strands per stator slot	63	67
b_{pc}	Pole core width (mm)	379	383
n_f	Number of turns per pole	36	36
b_{cuf}	Width of field winding (mm)	127	145.3
δ	Airgap length (mm)	23.6	17.8
h_{cus}	Height of Roebel bar strand (mm)	1.6	1.6
h_{cuf}	Height of field winding turn (mm)	4.0	4.0
	Machine parameters:		
L	Length	2.34 m	1.93 m
η	Efficiency	98.85 %	98.87 %
U_n	Stator line voltage	9.012 kV	10.048 kV
A	Armature loading	801 A/cm	916 A/cm
B_δ	Airgap flux density	0.93 T	0.88 T
$m_{cu,s}$	Stator copper weight	9819 kg	10256 kg
$m_{cu,r}$	Rotor copper weight	15894 kg	15895 kg
$m_{Fe,s}$	Stator iron weight	60593 kg	51813 kg
$m_{Fe,r}$	Rotor iron weight	75770 kg	66630 kg
X'_d	Transient reactance	0.24 p.u.	0.32 p.u.
X''_d	Subtransient reactance	0.18 p.u.	0.24 p.u.

reduced, the flux pulsations in the pole shoe increases, leading to increased losses.

The airgap length is inversely proportional to the nominal frequency. Pole shoe losses are proportional to the value of the synchronous reactance (3), meaning that the pole shoe losses are proportional to the nominal frequency. When the frequency increases, the airgap length is reduced, resulting in a smaller airgap length to slot opening ratio. This leads to increased pole shoe losses. In conclusion, the pole shoe losses increase when the nominal frequency or the synchronous reactance increase.

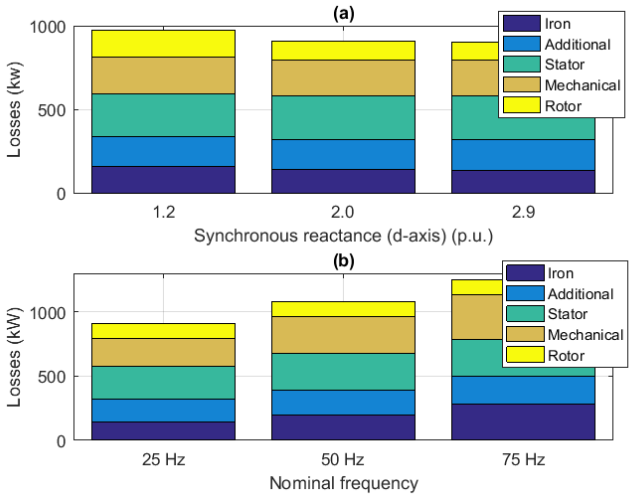

Fig. 10: Losses in the generator, (a) at 50 Hz, (b) at 2.0 p.u. synchronous reactance.

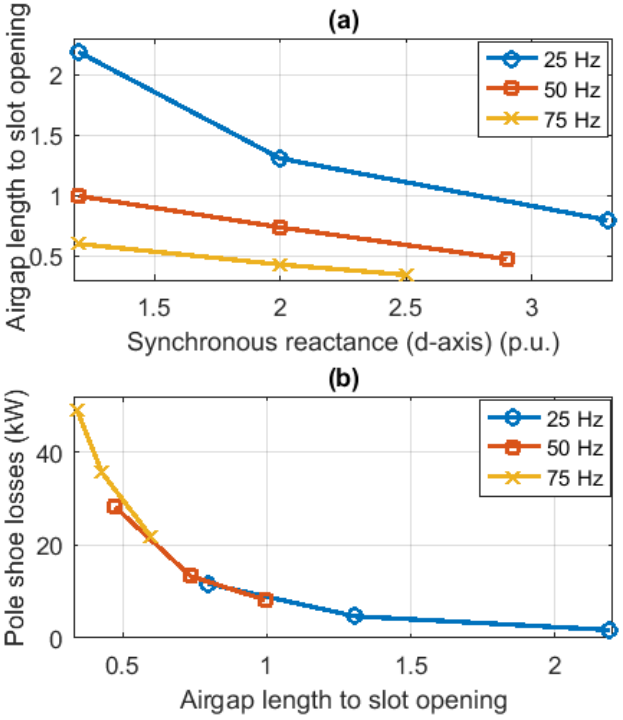

Fig. 11: Pole shoe losses, (a) airgap length to slot opening, (b) pole shoe loss estimate.

IV. Discussion of Results

When moving from one nominal frequency to another, two counter-acting cost effects are observed. Increasing the frequency will increase the losses and with it the capitalized cost of losses. Working to reduce the total cost, an increase in nominal frequency is reducing the amount of active materials needed, reducing the cost of materials. When the nominal

frequency was increased from 25 to 50 Hz, the reduction in the cost of materials was greater than the increase in loss cost. This made the 50 Hz designs cheaper than the 25 Hz designs. Moving fro 50 to 75 Hz reduced the cost of materials less than the increase in the cost of losses, giving an increase in the total generator cost. For the three nominal frequencies tested, the 50 Hz designs had lower total cost than the 25 and 75 Hz designs.

For the 75 Hz designs, the cost of losses are large compared to the cost of materials. In this paper, the same type of stator iron has been used for all nominal frequencies. If a nominal frequency of 75 Hz would have been chosen, it is likely that a higher quality stator iron with lower specific losses should have been chosen. By choosing an iron type with lower specific losses, the cost of materials will increase, but the cost of losses would decrease. It is likely that the cost of losses would decrease more than the cost of materials would increase, leading to a lower total generator cost. This would in turn reduce the gap in total cost between the 75 Hz designs and the 25 and 50 Hz designs, making the 75 Hz designs more attractive and possible push the optimal nominal frequency above 50 Hz.

Increasing the value of the synchronous reactance from 1.2 p.u. to 2 p.u. reduces the total generator cost with 4.49 to 5.62 %. The lower the nominal frequency, the higher the cost reduction. This can be attributed to the length of the airgap, in that a larger reduction in airgap length gives a larger cost reduction.

Increasing the synchronous reactance even more gives a smaller cost reduction and several possible design issues that must be handled. When the upper limit on the synchronous reactance was removed, the cost was reduced 0.56 - 2.12 %. The cost benefits of increasing the synchronous reactance must be weighed against possible design issues. Based on the results presented here, it seems to be most beneficial to increase the synchronous reactance to 2.0 p.u.

V. Conclusions

For the given generator specifications - 25, 50 and 75 Hz were used as nominal frequencies in the optimization. The main conclusions of the paper are:

1) the total generator cost is reduced when the synchronous reactance is increased.
2) the lowest total cost of the 50 Hz designs are lower than the cost of the 25 and 75 Hz designs.

The designs using 50 Hz were found to be cheaper than all other designs. Moving from 25 Hz to 50 Hz reduces the cost of materials more than the cost of losses are increased. When moving from 50 to 75 Hz, the reduction in materials cost is smaller than the increase in the cost of losses.

Increasing the synchronous reactance from 1.2 p.u to 2.0 p.u. reduced the total cost of the generator. The largest cost reduction was achieved with the lowest nominal frequency.

Increasing the synchronous reactance above 2.0 p.u. led to a smaller reduction in total cost than the reduction achieved by lifting the upper reactance limit from 1.2 p.u. to 2.0 p.u. Several design issues might become apparent when the synchronous reactance is increased. The benefit of cost reduction must be weighed against the negative effects when the final value of the synchronous reactance is chosen.

Increasing the value of the synchronous reactance from 1.2 p.u. to 2.0 p.u. has been shown to reduce the total cost of the generator. This reduction in cost can help offset parts of the cost of the converter that is associated with having a converter-fed synchronous hydrogenerator in pumped-storage plants. This can in turn make variable-speed pumped storage plants more cost competitive versus traditional fixed-speed solutions.

References

[1] M. Valavi and A. Nysveen, "Variable-Speed Operation of Hydropower Plants: Past, Present, and Future," in *2016 XXII International Conference on Electrical Machines (ICEM)*, Sept 2016, pp. 640–646.

[2] C. E. Stephan and Z. Baba, "Specifying a turbogenerator's electrical parameters guided by standards and grid codes," in *Electric Machines and Drives Conference, 2001. IEMDC 2001. IEEE International*, 2001, pp. 63–68.

[3] J. M. Fogarty, "Connections between generator specifications and fundamental design principles," in *Electric Machines and Drives Conference, 2001. IEMDC 2001. IEEE International*, 2001, pp. 51–56.

[4] A. B. M. Aguiar and A. Merkhouf and C. Hudon and K. Al-Haddad, "Influence of the Variation of the Input Parameters on the Simulation Results of a Large Hydrogenerator," *IEEE Transactions on Industry Applications*, vol. 50, no. 1, pp. 261–268, Jan 2014.

[5] G. Traxler-Samek and T. Lugand and A. Schwery, "Additional Losses in the Damper Winding of Large Hydrogenerators at Open-Circuit and Load Conditions," *IEEE Transactions on Industrial Electronics*, vol. 57, no. 1, pp. 154–160, Jan 2010.

[6] N. Stranges and J. H. Dymond, "How design influences the temperature rise of motors on inverter drives," *IEEE Transactions on Industry Applications*, vol. 39, no. 6, pp. 1584–1591, Nov 2003.

[7] P. Rasilo and A. Belahcen and A. Arkkio, "Effect of Rotor Pole-Shoe Construction on Losses of Inverter-Fed Synchronous Motors," *IEEE Transactions on Industry Applications*, vol. 50, no. 1, pp. 208–217, Jan 2014.

[8] E. L. Engevik and A. Røkke and R. Nilssen, "Evaluating hybrid optimization algorithms for design of a permanent magnet generator," in *ACEMP 2015 Optim - Electromotion Joint Conference*, Sept 2015, pp. 711–718.

[9] J. Pyrhönen, T. Jokinen, and V. Hrabovcová, *Design of Rotating Electrical Machines*, 2nd ed. John Wiley & Sons, Ltd, 2014.

[10] E. L. Engevik, M. Valavi, and A. Nysveen, "Efficiency and loss calculations in converter-fed synchronous hydrogenerator," in *2016 XXII International Conference on Electrical Machines (ICEM)*, Sept 2016, pp. 1636–1642.

[11] P. Kundur and N. J. Balu and M. G. Lauby, *Power system stability and control*. McGraw-hill, 1994.

[12] Statnett SF, "Veileder - Funksjonskrav i kraftsystemet 2012 (In Norwegian)," *Norwegian grid codes for transmission system*, 2012.

[13] I. Boldea, *Synchronous generators*, 2nd ed. CRC Press, 2015.

[14] D. Liu and H. Polinder and X. Wang and J. A. Ferreira, "Evaluating the cost of energy of a 10 MW direct-drive wind turbine with superconducting generators," in *2016 XXII International Conference on Electrical Machines (ICEM)*, Sept 2016, pp. 318–324.

[15] J. K. Nøland, "Fast-response rotating brushless exciters for improved stability of synchronous generators," *Licentiate thesis, Uppsala University*, 2016.